4. *Шумлянський Л., Деревська К.* Перші Sm-Nd та Rb-Sr ізотопно-геохімічні дані стосовно вендських базальтів Волині // Наук. праці Ін-ту фундамент. досліджень. – Київ: Знання, 2001. – С. 67–75.

5. *Носова А. А., Веретенников Н. В., Левский Л. К.* Природа мантийного источника и особенности коровой контаминации неопротерозойских траппов Волынской провинции (Nd – и Sr-изотопные и ICP-MS геохимические данные) // Докл. АН. – 2005. – **401**, № 3. – С. 429–433.

6. *DePaolo D. J.* Neodymium isotopes in the Colorado Front Range and crust-mantle evolution in the Proterozoic // Nature. – **291**. – P. 193–196.

7. *Claesson S., Bogdanova S. V., Bibikova E. V., Gorbatschev R.* Isotopic evidence for Paleoproterozoic accretion in the basement of the East European Craton // Tectonophys. – 2001. – **339**. – P. 1–18.

8. *Skridlaite G., Baginski B., Whitehouse M.* The ca 1.5 Ga zircons and monazites in charnockites from the western East European Craton // Geoph. Res. Abstracts. – 2006. – **8**, No 07385.

9. *Bogdanova S.* The East European craton: some aspects of the Proterozoic evolution in its south-west: Crystalline rocks of the East-European craton. Scientific communications of the 12th meeting of the Petrology group of the Mineralogical Society of Poland // Miner. soc. Poland. – 2005. – **26**. – P. 18–24.

10. *Krzeminska E., Williams I., Wiszniewska J.* A late Paleoproterozoic (1.80 Ga) subduction-related mafic igneous suite from Lomza, NE Poland // Terra Nova. – 2005. – No 17. – P. 442–449.

11. *Condie K. C.* Mantle plumes and their record in Earth history. – Cambridge: Cambridge Univ. Press, 2001. – 306 p.

Институт геохимии, минералогии
и рудообразования НАН Украины, Киев
Институт геологии рудных месторождений,
петрографии, минералогии и геохимии РАН, Москва

UDC 539.3

© **2008**

V. O. Vakhnenko, O. O. Vakhnenko, J. A. TenCate, T. J. Shankland

Quasistatic loading of Berea sandstone

(Presented by Corresponding Member of the NAS of Ukraine V. A. Danylenko)

Запропонована феноменологічна модель для опису властивостей напруження-деформація пісковика під дією повільного навантаження. Розглянута комбінація трьох механізмів, які пов'язуються з внутрішніми обмінними процесами: механізм стандартного релаксуючого твердого тіла, пружний механізм з прилипанням, механізм залишкової пластичної деформації. З малою кількістю параметрів модель відтворює як якісно, так і кількісно головні експериментальні дані по напруженню-деформації для пісковика Береа. Модель правильно відтворює великі та малі петлі на траєкторії напруження-деформація (пам'ять про кінцеву точку). Власне запропонована залежність деформації від напруження є не чим іншим, як рівнянням стану пісковика.

The measurements of typical stress-strain dependences for rocks under quasistatic loading point out their essentially nonlinear behavior. The results by Boitnott [1], Hilbert et al. [2] and Darling et al. [3] on repeatable hysteretic loops in stress-strain curves are well known. In essence, modeling the stress-strain dependences reproduces the sandstone state equation. Dealing only with macroparameters such as stress and strain while the processes on a microlevel still remain unknown makes it very difficult to create a model that adequately describes these properties. Recent experiments [3] showed that the most remarkable stress-strain properties of rocks are
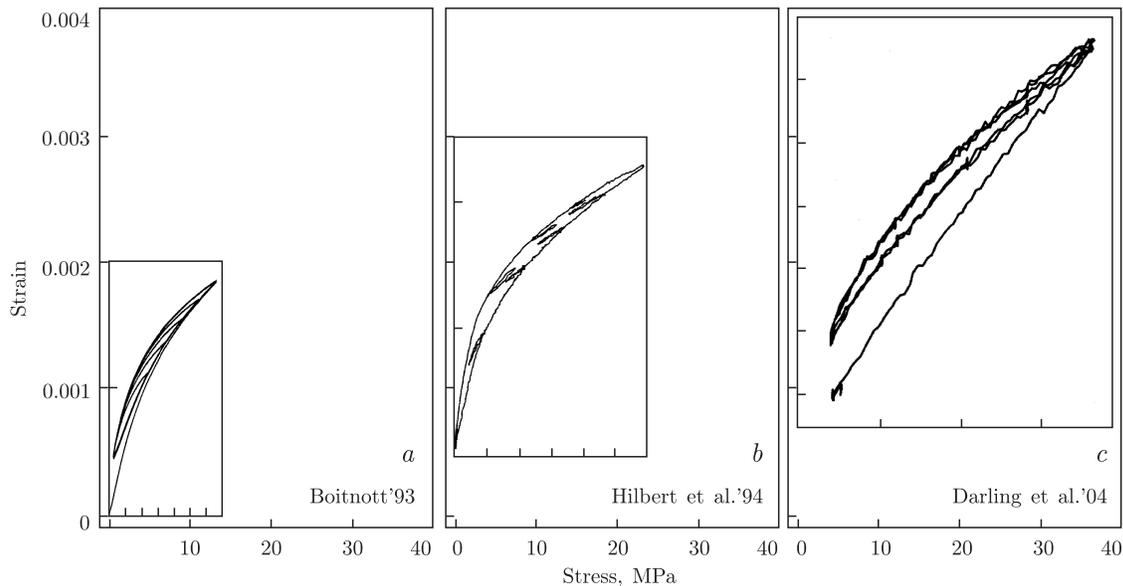
Fig. 1. Experimental results for Berea sandstone: (*a*) Boitnott [1], (*b*) Hilbert et al. [2], (*c*) and Darling et al. [3]. Stress-strain trajectories with their original coordinate meshes are placed within common coordinates. The systematic strain shifts caused by the apparatus adjustments are zero for Boitnott data, 0.00042 for Hilbert et al. data, and 0.00097 for Darling et al. data

determined by a small volume of material at grain contacts. However, it is unclear how interior equilibration processes in rocks under quasistatic loading can be studied in detail. In the literature there are a number of models that qualitatively describe the relationships between macroparameters such as stress and strain. First of all, there are two models, the Hertz–Mindlin model [4] and the Preisach–Mayergoyz model [5]. However, with these approaches, there is some difficulty in assigning a set of model hysteretic elements to real physical processes. While these approaches can duplicate experimental observations, their incompletely formulated connection between the distribution of auxiliary elements and maximum stress levels leads to limited predictive power.

We suggest three appropriately formalized mechanisms [6] that appear to actually occur in rocks under quasistatic loading: (i) a "standard solid relaxation" mechanism [7], (ii) a "sticky-spring" mechanism, and (iii) a "permanent plastic deformation" mechanism. A suitable combination of these mechanisms enables us to derive some general stress-strain relations, although without a detailed description of interior equilibration processes. As a result, we can obtain a phenomenological model that allows us to simulate qualitative and quantitative stress-strain characteristics and to reproduce the distinctive features typical of the basic experimental observations by Boitnott [1], Hilbert et al. [2], and Darling et al. [3] for Berea sandstone.

1. Observation of experimental data. In order to facilitate the analysis of three groups of fundamental experimental data for Berea sandstone by Boitnott (Fig. 1 in [5]), Hilbert et al. (Fig. 2 in [5]), and Darling et al. (Fig. 1 in [3]), we place them in a common presentation. Because, in different experiments, the origins of strain coordinates were introduced in different ways, it is an advantage to combine all experimental stress-strain curves into a single format. We proceed from the assumption that, for all three experimental curves, the points relating to maximum stress should be placed somewhere on the longest of available unconditioned curves, i. e., on the
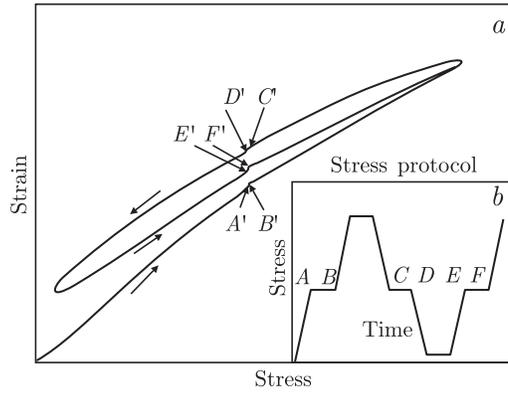
Fig. 2. Features of the stress-strain relations for Meule sandstone [3] (qualitative picture)

bottom curve of Fig. 1c, while the origin for the common strain coordinate should be chosen from Fig. 1a, where the starting point of the unconditioned (bottom) curve is documented. In this terminology, the word "unconditioned" refers to an initial curve that starts at zero stress on a sample that has been undisturbed for a long period (of the order of many hours or a day) as is the case in Fig. 1a. In contrast, the curves of Fig. 1b are "conditioned", that is, have undergone multiple stress cycles. In this case, the starting point is not shown and, except for the final, highest point, the unconditioned curve is absent. The original experimental figures have different scales, and, in Fig. 1, we have placed the experimental curves (omitting the scale numbers for clarity) into common coordinates. In this procedure, Fig. 1a preserves its coordinates, while Fig. 1b and Fig. 1c are shifted to include zero strain positions; the strain shift is zero for Fig. 1a, 0.00042 for Fig. 1b, and 0.00097 for Fig. 1c.

It is pertinent to note that this approach for introducing common coordinates is not ideal inasmuch as it essentially treats the actual position of the initial (unconditioned) curve as independent of the rate of increase of the applied stress, which in general is not the case. However, experimentally such a rate dependence is mainly detectable at high stresses and can be neglected in the first (but rather good) approximation without practical consequences within the common frame of reference.

The first effect that arises from a detailed analysis of experimental data as in Fig. 1 is the manifestation of some internal relaxation process that appears as a characteristic loop-like retardation in the strain response upon external loading and unloading stresses. Recently we discussed the relaxation mechanism for sandstones in terms of a phenomenological standard solid relaxation mechanism that arises from a nonlinear generalization [8] of the well-established relaxation modeling in the framework of a standard linear solid [9] (also see [7] and references therein).

Second, stress cycling gives rise to hysteresis loops in stress-strain curves. Observing the experimental dependences from [3] (particularly Fig. 1 in [3]) reveals that opposite sides of each loop are not entirely stuck together even at an infinitely slow loading, that is, the loops persist independently of loading time. Hence, there must be specific irreversible interior changes responsible for the loop formation, i. e., ones that can not be attributed simply to relaxation. We presume that some sort of friction has to be involved in any mechanism responsible for this effect. Therefore, we are forced to take a second mechanism, referred to here as a sticky-spring mechanism, into account for describing this aspect of sandstone stress-strain properties.

Finally, the whole treatment would be incomplete without including the third mechanism termed permanent plastic deformation. This third mechanism is needed to explain the observation that unconditioned and conditioned experimental curves differ from each other due to a permanent deformation, that is, a strain offset.

The next section provides a comprehensive treatment of these three mechanisms in order to model the interior processes that arise in rock samples under quasistatic compression.

2. Model approaches. This paper treats the uniaxial compression of a rock sample restricted to quasistatic loading. In this (slow loading) approximation, the stress σ turns out to be uniform along a sample and is determined by the absolute value of the external loading which plays the role of an external governing parameter. For the latter reason, we assign both σ and strain ε to be positive quantities as they are usually regarded in quasistatic compression experiments.

The fact that it is sufficient to operate directly with the stress-strain relation for the interpretation of quasistatic experiments provides a good basis for understanding the main mechanisms of inelasticity and elasticity, especially nonlinear ones, as well as allows one to formalize and verify these mechanisms. As mentioned above, we consider separately three mechanisms to account for interior processes in a rock sample under quasistatic loading: (i) standard solid relaxation, (ii) sticky-spring, and (iii) permanent plastic deformation.

2.1. Standard solid relaxation mechanism. The first part ε^r of the total strain ε to be considered is a relaxation mechanism caused by an interior equilibration process. We use the superscript index r to distinguish ε^r from other contributions to ε. According to the experimental curves in Section 1, ε^r may depend on time not only implicitly through the governing stress σ but also explicitly through relaxation. Thus, in general, strain can have different values at the same stress. However, the main hypothesis, which will be confirmed *a posteriori*, consists in assuming that strain also responds to the stress variation in time, or more precisely, to its time derivative $\dot{\sigma}$. The relaxation mechanism has been described in detail in [7], from which we use relations (2)–(5). The model incorporated in the dynamical state equation (2) in [7] is termed the standard solid relaxation mechanism in view of its generic property of interconnection of two different nonlinear elastic state equations that are mediated through hidden interior relaxation processes, just as two linear state equations are interconnected in the theory of a standard linear solid.

We observe, as is noted in [7], that modeling the Boitnott's experiments leads to almost ideal results. In contrast, the Hilbert's experiment cannot be adequately described solely by relaxation, inasmuch as it does not close the small loops through the stress-strain cusps for any assignment of constants in the state equations. The relaxation mechanism by itself does not explain end-point memory [6, 7].

2.2. Sticky-spring mechanism. In order to develop a means to explain the end-point memory of the stress-strain curves mentioned above, it helps to examine the stress-strain curves for Meule sandstone in [3]. For this purpose, we select only important parts of these data and depict them qualitatively in Fig. 2. Points corresponding to each other in the stress protocol picture (Fig. 2b) and the stress-strain picture (Fig. 2a) are marked by the same capital letters and are unprimed and primed, respectively. In the time intervals AB, CD, and EF, stress is constant. The fact that points A', C', and E' do not coincide with the respective points B', D', and F' could be explained by relaxation alone. However, relaxation by itself should inevitably lead the experimentally distinct points D' and F' (and even B') to coincide. To resolve this problem and understand the discrepancy, it is necessary to include an additional mechanism,
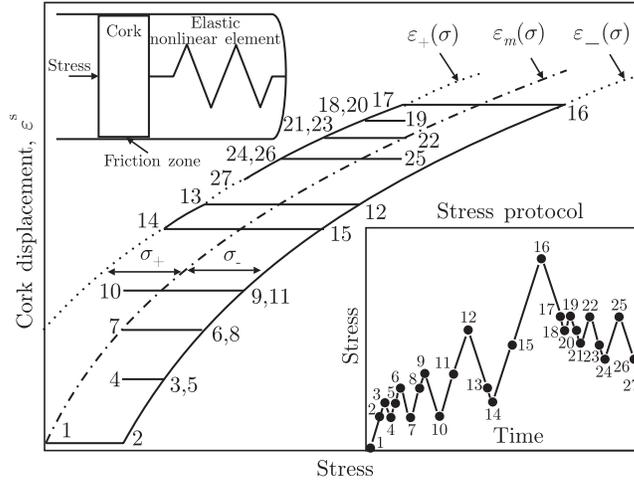
Fig. 3. Analog model to illustrate the sticky-spring mechanism in the upper left corner and its stress protocol in the lower right corner. Shown is the cork displacement ε^s in response to external loading σ. The curve of medial equilibrium $\varepsilon = \varepsilon_m^s(\sigma)$ is marked by a dash-dotted line

the sticky-spring mechanism, and, for the sake of convenience, to formulate it separately from the other mechanisms.

A prototype system to illustrate this mechanism is given in the left upper corner of Fig. 3. The system consists of a cylinder containing a cork plug and an elastic nonlinear element. In the sticky-spring mechanism, we invoke the friction between a plug and tube walls along with the elastic restoring force supplied by the elastic nonlinear element. The maximum frictional force is taken to be proportional to the threshold stresses $\sigma_\mp$ (positive values) that must be overcome by external stress σ against an internal elastic force (or vice versa) in order for the cork plug to be pushed from one position into another. In terms of the stress-strain variables, we postulate the principal features of the sticky-spring mechanism as follows:

$$\frac{d\varepsilon^s}{dt} = \theta(\dot{\sigma})\theta(\varepsilon_-(\sigma) - \varepsilon^s)\frac{d\varepsilon_-}{d\sigma}\dot{\sigma} + \theta(-\dot{\sigma})\theta(\varepsilon^s - \varepsilon_+(\sigma))\frac{d\varepsilon_+}{d\sigma}\dot{\sigma}. \tag{1}$$

Here $\theta(z)$ is the Heaviside step function. The partial strain ε^s is associated with the sticky-spring contribution to the total strain ε, while the functions $\varepsilon_-(\sigma)$ and $\varepsilon_+(\sigma)$ are determined via the medial equilibrium state function $\varepsilon_m^s(\sigma)$ and two positive threshold stresses σ_+ and σ_- as follows:

$$\varepsilon_-(\sigma) \equiv \varepsilon_m^s(\sigma - \sigma_-), \qquad \varepsilon_+(\sigma) \equiv \varepsilon_m^s(\sigma + \sigma_+). \tag{2}$$

We note that no restrictions are imposed on the threshold values σ_- and σ_+ that are responsible for the friction. In principle, they can be functions of stress σ.

Some aspects of the sticky-spring mechanism are presented in Fig. 3, which illustrates the dependence of sample strain ε^s on stress σ. For this purpose, Eq. (1) has been numerically integrated from the initial condition $\varepsilon^s(t = 0) = 0$ using the pressure protocol given in the right lower corner of Fig. 3. The essential feature of the sticky-spring mechanism consists in producing a stripe-like horizontal continuum of stationary states between the curves $\varepsilon^s = \varepsilon_-(\sigma)$ and $\varepsilon^s = \varepsilon_+(\sigma)$ as in Fig. 3. Only in the limit of very small threshold stresses ($\sigma_- \to +0$, $\sigma_+ \to +0$) do these curves come together and give rise to a single curve $\varepsilon^s = \varepsilon_m(p)$. This medial curve turns out to bisect the stripe and can be thought as the equilibrium curve of the process

in the limiting case of $\sigma_- \to +0$, $\sigma_+ \to +0$. Another essential part of this mechanism is its elastic component manifested through the inclination of each envelope curve $\varepsilon_-(\sigma)$ and $\varepsilon_+(\sigma)$ with respect to the stress axis.

For the function $\varepsilon_m^s(\sigma)$, we assume $\varepsilon_m^s(\sigma) = \varepsilon_e^r(\sigma)$, where $\varepsilon_e^r(\sigma))$ is determined by Eqs. (2)–(4) from [7]. In accord with thermodynamic principles, this relation thus requires that the final position of a true equilibrium state be independent of the origin of the internal processes that led to this equilibrium.

In Section 3 we show that, in the proper combination, the standard solid relaxation mechanism and the sticky-spring mechanism enable us to model both relaxation steps on conditioned curves under a fixed load (Fig. 2) and end-point memory, respectively. However, to include the unconditioned portion of the curves, we must invoke a mechanism that takes plastic deformation into account.

2.3. Permanent plastic deformation mechanism. Taking the intuitively understandable features of permanent plastic deformation into account, we postulate that, under compression, i.e., during increasing initial loading $\dot\sigma > 0$, the sample must contract, on the one hand, with a permanent plastic contribution ε^p to total strain to obey a linear Hooke-like law $\varepsilon^p = \sigma/E_p$ (where the appropriate Young modulus E_p is presumed to be stress-independent). On the other hand, it must simultaneously experience interior irreversible deformations. Conversely, when external loading decreases, $\dot\sigma < 0$, the plastic component ε^p must remain fixed. To formalize the statements above, the state equation for the permanent plastic deformation mechanism can be described as

$$\frac{d\varepsilon^p}{dt} = \theta(\dot\sigma)\theta\left(\frac{\sigma}{E_p} - \varepsilon^p\right)\frac{\dot\sigma}{E_p}. \tag{3}$$

According to this mechanism, once a peak loading is achieved, the possible store of plastic deformation in the rock sample becomes saturated. Thereafter, when loading less than the peak stress, the permanent plastic deformation mechanism does not appear in subsequent cycles. Through the Heaviside function, only an unconditioned curve manifests permanent plastic deformation; on conditioned curves, it does not contribute.

The separation of the sticky-spring mechanism and the permanent plastic deformation mechanism can have a physical interpretation. In the experimental results [1, 2, 3] each increment of stress (starting at zero stress) beyond the previous highest stress produces irreversible changes in the rock fabric as crack surfaces slide and asperities are crushed. The permanent plastic mechanism is a means of incorporating these irreversible changes. In a regime where stress cycles at stresses less than the maximum previously achieved, the sticky-spring mechanism is applied. It may be that the Preisach–Mayergoyz approach [5] can cover the whole stress range, yet there is the utility in the present approach, where damaging stresses are separated from a regime in which stress cycles are associated with reversible changes in the rock.

Some additional details of the suggested mechanisms can be found in [6], in particular, the connection with the Preisach–Mayergoyz model [5].

3. Simulation of stress-strain relations. In previous sections, we suggested three mechanisms by which interior interaction processes in sandstones are assumed to take place. Because the physical origins of these processes have not been well established, we use a phenomenological approach in which they are not specifically defined. Taking all three developed mechanisms into account, we rely upon the minimum number of processes, i.e., only a single process for each

mechanism. For loading by a given stress protocol, we can solve Eqs. (1), (3) and (2)–(5) from [7] with the initial conditions $\varepsilon^r(t=0) = \varepsilon^s(t=0) = \varepsilon^p(t=0) = 0$ and find the total strain ε as a linear combination of partial strains:

$$\varepsilon = b(\varepsilon^r + \varepsilon^p) + (1-b)(\varepsilon^s + \varepsilon^p). \tag{4}$$

Here, the constant b is bounded inside the interval $0 \leqslant b \leqslant 1$. Thus, at $b = 1$ we have the relaxation mechanism with permanent plastic deformation only, while, at $b = 0$, we retain only the sticky-spring mechanism plus a permanent plastic deformation. Choosing relation (4) as a linear combination, we are able to tune the single parameter b to obtain a physical condition such that the true equilibrium state is independent of any one type of interior relaxation process.

If the stress is fixed at one moment, then the relaxation mechanism moves the whole system to some new equilibrium during a characteristic relaxation time. Owing to the sticky-spring mechanism plus the permanent plastic deformation mechanism, there can be several equilibrium states at the same stress. The ambiguity of the equilibrium state dependence on stress can be found in [10].

The best fit of the calculated results as applied to all three groups of experiments on Berea sandstone [1, 2, 3] (see also Fig. 1) was obtained with the parameters listed in Table 1. The parameters τ, E_e^-, E_e^+, D, and a are assigned for Eqs. (2)–(5) in [7].

Figure 4 presents the results of numerical simulations. Comparing the calculated curves (Fig. 4) with experimental data (Fig. 1), we observe an acceptable coincidence of these results both qualitatively and quantitatively. First, we find the small loops in curve *2* of Fig. 4 that model the experiment of Hilbert et al. [2]. These loops are closed at the cusps. Although the time relaxation is small, the relaxation mechanism cannot be completely removed because it plays an important role in describing the end-point memory; this effect is manifested by the small loops on the theoretical curve *2* in Fig. 4, which reproduce the experiment of Hilbert et al. [2]. On the one hand, it is precisely the effect of small but finite relaxation time that enables one to close a small loop through a cusp (see curve *2* in Fig. 4 once again). On the other hand, the relaxation provides the means to produce the small loops in the modeling.

4. Conclusion. A phenomenological model to describe the stress-strain properties of Berea sandstone under quasistatic loading is suggested. Analysis of experimental observations has demonstrated the need to invoke several mechanisms that are responsible for interior equilibration processes in sandstone: the standard solid relaxation mechanism, the sticky-spring mechanism, and the permanent plastic deformation mechanism [6]. To justify these mechanisms, we have used an approach in which the interior processes in a sample are not explicitly defined, which simplifies drastically the mathematical description. Only by properly combining all three mechanisms are we able to obtain acceptable models. The resulting treatment reproduces extremely complex stress-strain trajectories with only nine adjustable parameters.

Because of the proposed treatment of quasi-static stress-strain relations, it becomes possible to realize an adequate and self-consistent simulation that describes both qualitatively and quantitatively the principal features of complex experimental data by Boitnott [1], Hilbert et

Table 1. Fitting parameters

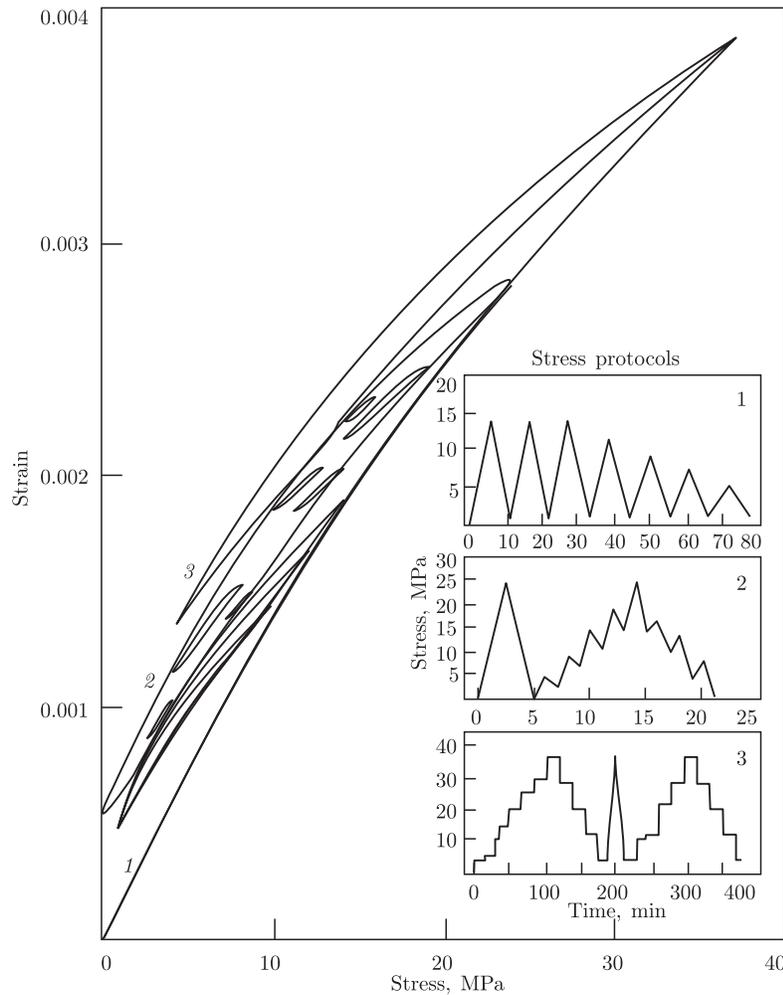| τ, s	E_e^-, GPa	E_e^+, GPa	D, MPa^{-1}	σ_-, MPa	σ_+, MPa	E_p, GPa	a	b
3	5	23	0.03	4	4	70	0.2	0.8

Fig. 4. Computer modeling of stress-strain trajectories for Berea sandstone. Curve *1* relates to the Boitnott experiment [1], curve *2* models the Hilbert et al. [2] experiment, and curve *3* reproduces the Darling et al. experiment [3]

al. [2], and Darling et al. [3] for Berea sandstone and, in particular, the details of end-point memory.

1. *Boitnott G. N.* Fundamental observations concerning hysteresis in the deformation of intact and jointed rock with applications to nonlinear attenuation in the near source region // Proc. Numer. Model. Underground Nuclear Test Monitor. Symp. – 1993. – LA-UR – 93–3839. – P. 121–137. – [Los Alamos Natl. Lab. Rep.].
2. *Hilbert jr. L. B., Hwong T. K., Cook N. G. W. et al.* Effects of strain amplitude on the static and dynamic nonlinear deformation of Berea sandstone // Rock mechanics models and measurements challenges from industry / Ed. by P. P. Nelson and S. E. Laubach. – Rotterdam, Netherlands. – 1994. – P. 497–515.
3. *Darling T. W., TenCate J. A., Brown D. W. et al.* Neutron diffraction study of the contribution of grain contacts to nonlinear stress-strain behavior // Geophys. Res. Lett. – 2004. – **31**. – L16604.
4. *Nihei K. T., Hilbert jr. L. B., Cook N. G. W. et al.* Frictional effects on the volumetric strain of sandstone // Int. J. Rock Mech. Min. Sci. Geomech. Abstr. – 2000. – **37**. – P. 121–132.

5. *Guyer R. A., McCall K. R., Boitnott G. N. et al.* Quantitative implementation of Preisach-Mayergoyz space to find static and dynamic elastic moduli in rock // J. Geophys. Res. – 1997. – **102**. – P. 5281–5293.

6. *Vakhnenko V. O., Vakhnenko O. O., TenCate J. A. et al.* Modeling of stress-strain dependences for Berea sandstone under quasi-static loading // Phys. Rev. B. – 2007. – **76**. – P. 184108(8).

7. *Вахненко В. О., Вахненко О. О., Даниленко В. А.* Релаксаційна модель механічної поведінки пісковика при квазістатистичному навантаженні // Доп. НАН України. – 2007. – № 7. – С. 109–115.

8. *Vakhnenko V. O.* High frequency soliton-like waves in a relaxing medium // J. Math. Phys. – 1999. – **40**. – P. 2011. – 2020.

9. *Zener C.* Elasticity and Anelasticity of Metals. – Chicago: Univ. Chicago Press, 1948. – 170 p.

10. *Gusev V. E., Lauriks W., Thoen J.* Dispersion of nonlinearity, nonlinear dispersion, and absorption of sound in micro-inhomogeneous materials // J. Acoust. Soc. Am. – 1998. – **103**. – P. 3216–3226.

Subbotin Institute of Geophysics,
Ukrainian Academy of Sciences, Kiev, Ukraine
Bogolyubov Institute for Theoretical Physics,
Ukrainian Academy of Sciences, Kiev, Ukraine
Los Alamos National Laboratory, Los Alamos,
New Mexico, USA